JOURNAL OF MATERIALS SCIENCE 33 (1998) 4101–4104

Measurement of the hardness distribution in sapphire/NiAl composites using continuous indentation

D. E. BOSS
Northwestern University, 1801 Maple Avenue, Evanston, IL 60201, USA
E-mail: danboss@concentric.net

A variety of fibre coatings have been modelled as a means to reduce the thermal residual stresses in sapphire/NiAl composites, including the use of molybdenum as a compliant layer. However, no experimental studies have been performed to quantify the effect of these coatings on the residual stresses. Measuring the effect of the coatings in real composites is a difficult task given the limitations of the most common residual stress measurement methods, such as X-ray and neutron diffraction. In this study, a continuous indentation system was used to measure a spatial hardness distribution both within the molybdenum fibre coatings and the NiAl matrix. Because it has been shown that residual stresses effect the apparent hardness of a material, the hardness distribution should be indicative of the local residual stress state in the sample. The measured hardness distributions showed distinct trends, including an increasing hardness in the molybdenum as the NiAl interface is approached, a substantial increase in NiAl hardness at the fibre/coating boundary, and a decrease in NiAl hardness that is proportional to the distance from the fibre/coating boundary. The potential utility of continuous indentation systems for mapping the residual stresses in composites is briefly discussed.

1. Introduction

The development of finite element models for the prediction of residual stress distributions in composite systems has greatly increased the number of research efforts to examine the effect of fibre coatings on composite performance. A limitation in these efforts is the lack of a method to measure the spatial stress distribution in the composite. Both neutron and X-ray diffraction are powerful tools for measuring residual stress in materials, but each suffers from limitations for measuring stresses in composites [1–3]. Neutron diffraction (ND) provides volume average strains in the composite, and provides very valuable information on the state of the reinforcement, and, if the volume fraction is high enough, the fibre coating. However, because it measures volume averages, the residual stress gradient around the fibre cannot be determined. X-ray diffraction (XRD) samples a much smaller volume of material, and, therefore, can be used to measure stress gradients. But, because of its small sample volume and limited penetration depth, it is often necessary to remove significant portions of the matrix to examine the stresses near the fibre–matrix boundary region, which modifies the residual stress distribution. The development of continuous indentation (CI) systems, with milli-Newton (mN) indentation force levels, offers the opportunity to obtain a spatial distribution of the stress gradients around a fibre *in situ* and to compare the effects of fibre coatings on the residual stresses in composites. It is well known that residual stresses change the apparent hardness of a sample [4–7]. Therefore, if these CI systems can obtain spatial hardness distributions around the fibres, then it may be possible to relate the change in hardness to the residual stresses present in the composite. The focus of this effort is to determine if spatial hardness profiles can be obtained and if hardness measurements can be made within the fibre coatings themselves.

2. Experimental procedure

Sapphire fibre-reinforced NiAl (sapphire/NiAl) composites with molybdenum fibre coatings between 3 and 30 μm were selected for this study. The substantial residual stresses in the sapphire/NiAl system have been well documented [8–10]. Molybdenum has been identified as a candidate fibre coating for this system [11]. The low work-hardening coefficient of molybdenum makes it an attractive material for a compliant fibre coating. It has been proposed [12] that compliant fibre coatings will reduce the thermal residual stresses in the composite by plastically deforming to accommodate the thermal expansion mismatch strains between the fibre and matrix. The deposition of the molybdenum coatings on to the sapphire fibre has been described in a NASA report [13]. The sapphire/NiAl composites were prepared by NASA–Lewis

Research Center using the powder cloth method which has been described elsewhere [14]. After consolidation, composite samples were sectioned using a metallographic saw, ultrasonically cleaned in isopropanol, and then vacuum encapsulated in epoxy. After a 24 h cure, each of the samples was polished with the fibres perpendicular to the polished surface. The polishing sequence consisted of 240, 320, 400, and 600 grit SiC papers followed by a 3 μm diamond paste. The polished samples were mounted on to a magnetic sample holder by melting a small quantity of wax on the holder, pressing the metallographic mount on to the molten wax, and then allowing the assembly to cool.

The hardness measurements were performed using a UMIS-2000 Ultra Micro-Indentation System produced by CISRO, Australia, Division of Applied Physics. The UMIS-2000 is a force-driven static measuring device [15] for ultra micro-indentation. The indentor is driven into, and withdrawn from, the surface in a discrete series of steps up to a preset maximum load. As the indentor penetrates the surface, its depth is measured at each of the force steps. The UMIS-2000 is equipped with a Berkovich diamond pyramid indentor. A video microscope and an X–Y coordinate stage, with a minimum step size of 2.5 μm, are used to position the sample for indentation measurements. The UMIS-2000 is mounted on a vibration damping table to isolate the system from outside vibrations. The analysis software of the UMIS-2000 calculates an equivalent Vicker's hardness. The calculation of Vicker's Hardness Number (VHN) is performed at the maximum force applied by using the projected area of the Berkovich indentor, which has the same depth to area ratio of a Vicker's indentor.

With the purpose of this study to characterize the spatial stress distribution in the composite, CI measurements were made in arrays of up to 99 indentations (the maximum allowable with the system). In performing these CI tests, the initial indentation location is manually selected using the videomicroscope and X–Y coordinate stage. To obtain accurate hardness measurements, it is necessary to bring the working depth for the indentor into the linear response region for the displacement sensor. This is done by repositioning the indentor to a location between 50 and 100 μm away from the coordinates of the initial point in the array, with the direction and distance dependent upon the sample, and then setting the working depth by running this feature in the system program.

Once the working depth was established, the sample was repositioned to the desired starting position, and an array file was selected from a set of files created separately. The 11×9 and 10×10 arrays were most often used. In each of these arrays, a 10 μm spacing between indentations in each row and between each column was used. CI measurements were made using a maximum load of 20 mN, a series of 30 force steps during both loading and unloading (total of 60 steps), and a pause between indentations of 30 s. After the indentations were completed, a micrograph of the array is taken (Fig. 1) and the length of the normal between each indentation and the edge of the fibre was measured. When fibre coatings were present in the sample, the material in which the indentation was made (e.g. molybdenum or NiAl) is also recorded.

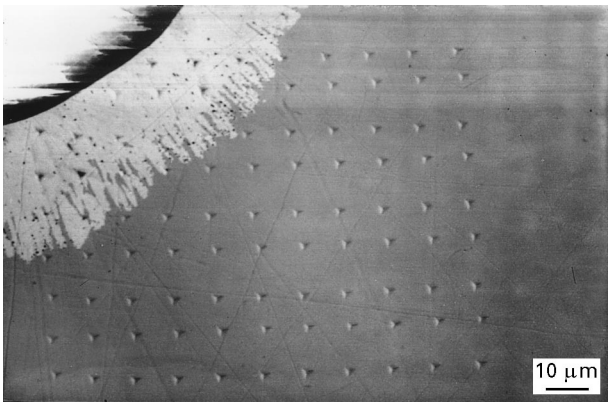

Figure 1 Typical CI measurement array in a 30 μm molybdenum sample.

3. Results

Four groups of samples were characterized in this effort; baseline composites, fibres with 3 μm molybdenum coatings, fibres with 10–15 μm molybdenum coatings, and fibres with 20–30 μm molybdenum coatings. For each type of sample, the hardness distribution around at least four different fibres were mapped. The data from each set of fibres for the selected coating thicknesses was combined and are presented in Figs 2–5 as summary plots of hardness versus distance from the fibre. The spatial hardness distributions were analysed via the curve-fitting feature included in the graphing software.

4. Discussion

4.1. Sapphire/NiAl

The summary plot of the hardness versus distance from the edge of the fibre for the baseline composite samples is shown in Fig. 2. This figure shows both the experimental data points and a calculated line fitted to the data. As a point of reference, a monolithic sample of NiAl was prepared by the powder cloth method and an average CI Vicker's hardness number (VHN) of 412 ± 30 was obtained. The hardness measurements show that the NiAl hardness is maximum adjacent to the fibre, decreases as the distance from the fibre interface is increased, and then reaches a plateau after a distance of approximately 35 μm. The calculated line is a compilation of two separate functions; a second-order polynomial fit for hardness values 30 μm or less from the fibre, and a linear fit for hardness values that are further than 30 μm from the fibre edge. The polynomial and linear equations are given in Equations 1 and 2, respectively

$$\mathrm{VHN} = 390 - 3.95X + 0.056X^2 \quad (1)$$

$$\mathrm{VHN} = 321.3 - 0.044X \quad (2)$$

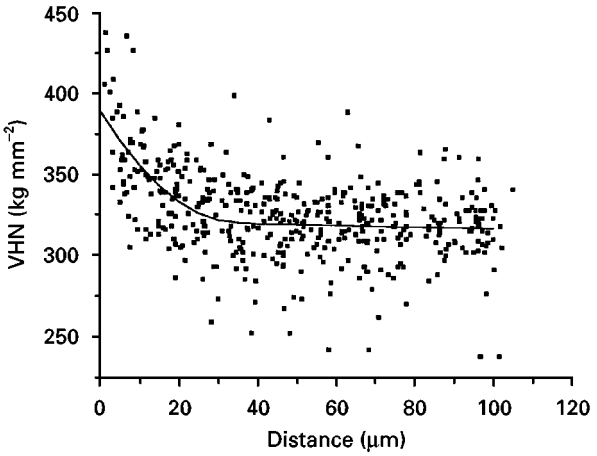

Figure 2 Summary of hardness versus distance from the sapphire fibre in baseline composite samples. (■) NiAl VHN, (—) fit VHN.

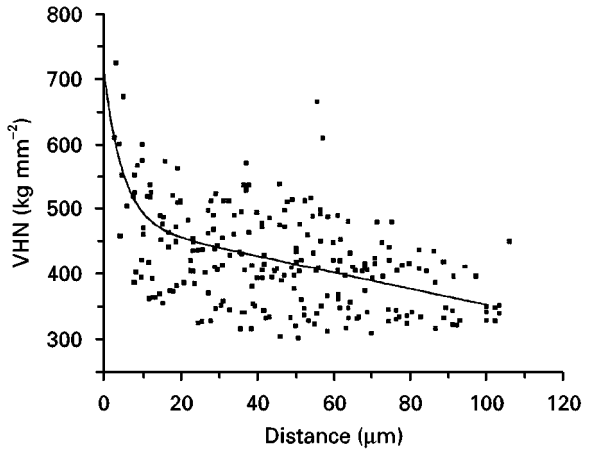

Figure 3 Summary of hardness versus distance from the sapphire fibre for composite samples with a 3 μm molybdenum fibre coating. (■) NiAl VHN, (—) fit VHN.

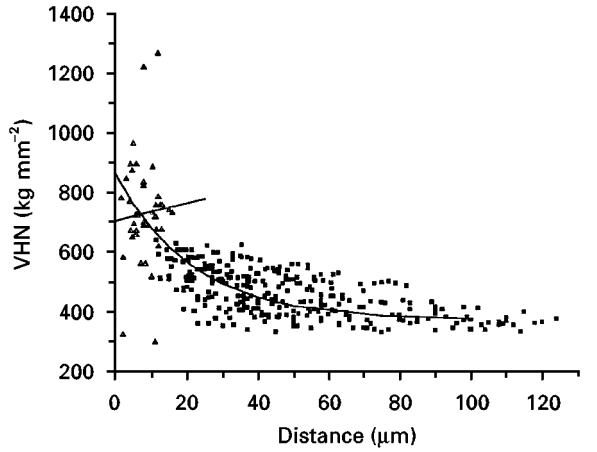

Figure 4 Summary of hardness versus distance from the sapphire fibre for composite samples with a molybdenum fibre coating of 10 and 15 μm. (■) NiAl VHN, (▲) Mo VHN, (—) NiAl fit, (- - -) Mo fit.

where X is the radial distance in micrometers from the edge of the sapphire fibre, and the VHN is in kg mm^{-2}. The data from these tests produce a relatively narrow band of hardness values, with the majority falling within $\pm 10\%$ of the calculated curve.

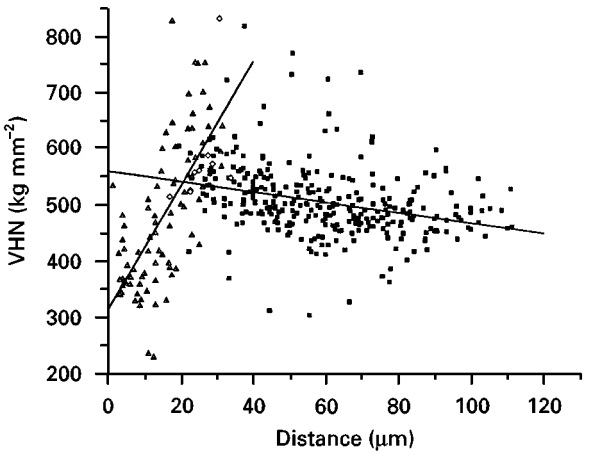

Figure 5 Summary of hardness versus distance from the sapphire fibre for composite samples with molybdenum fibre coatings of 20–30 μm. (■) NiAl VHN, (▲) Mo VHN, (◇) boundary VHN, (- - -) Mo fit, (—) NiAl fit.

4.2. Fibres with 3 μm molybdenum coatings

The summary plot of the hardness versus distance from the edge of the fibre for the composite samples with a 3 μm molybdenum fibre coating is shown in Fig. 3. The very thin molybdenum coatings in these samples did not allow hardness measurements for the fibre coating, so the data in Fig. 3 are only for the NiAl matrix. A distinct increase in the hardness of the NiAl is apparent in these results, compared both to an NiAl average VHN of 412 and the data summarized in Fig. 2. A VHN of the order of 600 was measured near the NiAl–Mo boundary with a sharp decrease within the first 10 μm before it becomes more linear. Converse to the baseline sample, no distinct plateau for the NiAl hardness is seen in Fig. 3. This figure shows both the experimental data points and a calculated line fitted to the NiAl data. The calculated line is an exponential decay function, which is given by

$$\text{VHN} = -2746.84 + 237.6e^{(-X/4.801)} + 3225e^{(-x/2488)} \quad (3)$$

where X is the radial distance in micrometres from the edge of the sapphire fibre.

4.3. Fibres with 10–15 μm molybdenum coatings

Hardness distributions from fibres with coatings between 10 and 15 μm are summarized in Fig. 4. This figure includes data for hardness values within the molybdenum coating as well as the NiAl matrix. The hardness values for the molybdenum coating were fitted using a linear regression function within the graphing software, while the NiAl data were fitted using an exponential decay function. The two equations are, respectively

$$\text{Mo VHN} = 706 + 2.9X \quad (4)$$

$$\text{NiAl VHN} = 372.35 + 492.45e^{(-x/21.44)} \quad (5)$$

where X is the radial distance from the edge of the sapphire fibre and the VHN are in kg mm^{-2}. The data

for the molybdenum coating are widely scattered with individual values from 300 VHN to over 1200 VHN. This wide variation introduces significant uncertainty for the utility of Equation 4. However, all of the hardness values for molybdenum are substantially higher than that reported for annealed molybdenum, which is typically a VHN in the range of 200–250. The data for the NiAl presents a much tighter fit to Equation 5. As with the previous samples, the hardness of the NiAl adjacent to the molybdenum region is significantly higher (600 VHN) than either the monolithic NiAl or baseline composite values. The hardness of the NiAl is inversely proportional to distance from the molybdenum boundary and appears to approach a limit at a distance of approximately 100 μm that is in good agreement with the monolithic NiAl hardness.

4.4. Fibres with 20–30 μm molybdenum coatings

The results of the CI measurements for the composite samples with molybdenum fibre coatings of between 20 and 30 μm are presented in Fig. 5. This figure shows the measured hardness values for both the NiAl matrix and the molybdenum fibre coating. For these samples, both the NiAl and molybdenum hardness values appeared to fit best to a linear regression function within the graphing software. Equations 6 and 7 provide the results of the linear regression fitting of the molybdenum and NiAl data, respectively

$$\text{Mo VHN} = 313.65 + 11.02X \quad (6)$$

$$\text{NiAl VHN} = 560.37 - 0.92X \quad (7)$$

where X is the radial distance in micrometres from the edge of the sapphire fibre and the VHN are in kg mm^{-2}. The data for the molybdenum coating presents a much more consistent fit with Equation 6 than the data for the 10 μm samples did with Equation 4. In the 20–30 μm molybdenum coatings, there is a clear trend of increasing hardness with increasing distance from the fibre edge. This indicates that the stress is reduced at the molybdenum–sapphire interface, but the mechanism for this cannot be determined solely from these measurements. The NiAl data are relatively tight fit with Equation 7, although there are a few outlying data points. The measured NiAl hardness at the molybdenum boundary does not change substantially from that observed for the 10–15 μm coatings or the 3 μm samples. For the data in Fig. 5, no hardness limit is apparent, as the distance from the fibre is increased in this sample.

5. Conclusion

The results from this initial evaluation of CI for measuring spatial hardness distributions show that the system is able to map the hardness distribution within both the fibre coating and the matrix. Given the experimental method of using an array of hardness measurements, fibre coatings may need to be greater than 5 μm thick for useful data to be obtained. The measured hardness values for both the molybdenum and NiAl show substantial increases in the microhardness of the materials compared to their bulk values, which indicates that significant residual stresses are present in the materials. Further, the hardness gradients found in both the molybdenum fibre coating and the NiAl matrix show that the CI method can provide spatial hardness resolution of the order of 5–10 μm. The thickness of the molybdenum coating does effect the hardness value measured in the coating and, to a lesser extent, the hardness distribution in the NiAl matrix. The ability of the CI method to obtain spatial hardness profiles within fibre coatings and in the adjacent matrix demonstrates the potential for obtaining residual stress profiles in composites using this method.

Acknowledgements

I thank Dr Randy Bowman, NASA – Lewis Research Center, for providing the composite samples and acting as project monitor on NASA – Lewis Research Center contract NAS3 – 26810 which produced the molybdenum coated sapphire fibres. I would also like to thank Professor Katherine Faber for her helpful discussions on the CI results. Special thanks go to my colleagues at Northwestern University, in particular Dr Jochen Schneider, for their assistance with the CI system.

References

1. I. C. NOYAN and J. B. COHEN, "Residual Stress-Measurement by Diffraction and Interpretation" (Springer, New York, 1987) p. 75.
2. T. M. HOLDEN and G. ROY, in "Handbook of Measurement of Residual Stresses", edited by J. Lu (The Fairmont Press, Lilliburn, GA, 1995) p. 133.
3. A. J. ALLEN, M. T. HUTCHINGS, C. G. WINDSOR and C. ANDREANI, *Adv. Phys.* **34** (1985) 445.
4. G. U. OPPEL, *Exp. Mech.* **4** (1964) 135.
5. T. R. SIMES, S. G. MELLOR and D. A. HILLS, *J. Strain Anal.* **19**(2) (1984) 135.
6. J. FRANKEL, A. ABBATE and W. SCHOLZ, *Exp. Mech.* June **33**(2) (1993) 164.
7. W. R. LaFONTAINE, C. A. PASKIET, M. A. KORHONEN and C.-Y. LI, *J. Mater. Res.* **6** (1991) 2084.
8. P. K. WRIGHT, M. D. SENSMEIR, D. KUPPERMAN and H. WADLEY, in "Hi Temp Review 1991", NASA Conference Proceeding 10082, edited by H. Gray (Nasa Lewis Research Center, Cleveland, OH, 1991) p. 45.1.
9. S. MAJUMDAR, J. P. SINGH, D. KUPPERMAN and A. D. KRAWITZ, *J. Eng. Mater. Technol.* **113** (1991) 51.
10. A. SAIGAL and D. KUPPERMAN, *Scripta Metall. Mater.* **25** (1991) 2547.
11. A. K. MISRA, K. S. CRANDALL and R. R. BOWMAN, in "NASA Conference Proceeding 10104", edited by H. Gray (Nasa Lewis Research Center, Cleveland, OH, October 1992) p. 39.1.
12. S. M. ARNOLD, V. K. ARYA and M. E. MELIS, *J. Compos. Mater.* **26** (1992) 1287.
13. D. E. BOSS, Final Report for NASA Contract NAS3-26810. Nasa Lewis Research Center, Cleveland, OH, 1993.
14. J. W. PICKENS, R. D. NOEBE, G. K. WATSON, P. K. BRINDLEY and S. L. DRAPER, NASA Technical Memorandum 102060, Nasa Lewis Research Center, Cleveland, OH (1989).
15. UMIS-2000 Operating Manual (CSIRO-Australia) Copyright March 1992.

Received 14 October 1997
and accepted 15 May 1998